

Preparation and Application of a Magnetic Composite ($\text{Mn}_3\text{O}_4/\text{Fe}_3\text{O}_4$) for Removal of As(III) from Aqueous Solutions

Gabriela Cordeiro Silva^{a,c}, Fabiana Soares Almeida^{b,c}, Angela Melo Ferreira^{b,c},

Virginia Sampaio Teixeira Ciminelli^{a,c*}

^aDepartment of Metallurgical and Materials Engineering,

Universidade Federal de Minas Gerais – UFMG, CEP 31270-901, Belo Horizonte, MG, Brazil

^bDepartment of Chemistry, Centro Federal de Educação Tecnológica de Minas Gerais – CEFET-MG, CEP 30421-169, Belo Horizonte, MG, Brazil

^cInstituto Nacional de Ciência e Tecnologia em Recursos Minerais, Água e Biodiversidade – INCT-Acqua, Belo Horizonte, MG, Brazil

Received: February 2, 2011; Revised: February 13, 2012

The introduction of magnetic properties in adsorbent materials has the aim of improving solid-liquid separation processes. In this work, a magnetic composite was synthesized through the precipitation of manganese oxide in the presence of magnetite particles using O_2 as an oxidant. The composite proved to be chemically and physically stable within a wide range of pH values. The composite characterization indicated that hausmannite (Mn_3O_4) represents the precipitated manganese phase and that magnetite undergoes no phase transformation during the synthesis. The composite and Mn_3O_4 particles were used to remove As(III) from aqueous solutions. The magnetic composite and Mn_3O_4 sample presented high and similar affinity for As(III), with maximum sorptive capacities of $14 \text{ mg}_{\text{As}} \text{ g}_{\text{solid}}^{-1}$ ($0.0048 \text{ mmol}_{\text{As}} \text{ m}^{-2}_{\text{solid}}$) and $20 \text{ mg}_{\text{As}} \text{ g}_{\text{solid}}^{-1}$ ($0.0049 \text{ mmol}_{\text{As}} \text{ m}^{-2}_{\text{solid}}$), respectively, at pH 5.0. The combination of an active high surface area sorbent (Mn_3O_4) with a magnetic phase (Fe_3O_4) allows for efficient As(III) removal and solid/liquid separation.

Keywords: magnetic composite, manganese oxide, arsenic, adsorption

1. Introduction

The presence of arsenic in drinking water is of great concern due to its toxicity and carcinogenic potential. Arsenic concentration below $10 \mu\text{g.L}^{-1}$ is the World Health Organization's (WHO) recommendation for drinking water supplies¹. The increasing water quality demand for human consumption and industrial support, coupled with stringent environmental legislation, has stimulated the development of new materials and methods for the treatment of arsenic-contaminated aqueous solutions. Adsorption processes are commonly present in water treatment. As desired features, adsorbents should be low-cost and should present a considerable contaminant adsorption capacity. When trace or sub-trace concentrations are of concern, powder adsorbents with small-sized particles and a large specific surface area are required. Separating small-sized particles of a highly specific surface area from a solution is a challenge that can be addressed with the use of magnetic adsorbents. Magnetic adsorbents can be conveniently recovered by magnetic separation, in turn avoiding the filtration steps, which represent a barrier to the application of high-performance, small-sized materials in environmental remediation processes and the treatment of great volumes of aqueous solutions. Some investigations have shown that magnetic iron oxides, such as magnetite nanoparticles, lead to the efficient removal of arsenic from contaminated water². Nevertheless, the instability of these magnetic nanoparticles

represents a problem, as magnetite is highly susceptible to oxidation when exposed to the atmosphere. To face this problem, magnetite nanoparticles are being combined with other compounds or covered by an active compound³⁻⁵. In both cases the magnetic property of magnetite is preserved.

The oxidation state and chemical speciation of arsenic play a determining role in its toxicity, mobility, and bioavailability in soil-water systems, the As(III) species being the most toxic and mobile. Under oxidizing conditions, H_2AsO_4^- is the dominant inorganic arsenic species at low pH (from pH 2.0 to pH 6.9), while at higher pH, HAsO_4^{2-} becomes dominant. The inorganic species H_3AsO_4 and AsO_4^{3-} may be present in extremely acidic and alkaline conditions, respectively. Under reducing conditions at a pH of less than approximately pH 9.2, the uncharged As(III) species H_3AsO_3 predominates⁶. The most used arsenic removal techniques, such as adsorption on activated alumina and coprecipitation with ferric salts, are often more effective for As(V) than for As(III) removal, given that the predominant As(III) species at circumneutral pH is the uncharged H_3AsO_4 , while for As(V) the predominant species are the charged H_2AsO_4^- and HAsO_4^{2-} ^[6]. Therefore, an oxidation step is often used to improve arsenic removal and fixation. Manganese oxides are known as effective oxidizers of As(III) to As(V) in natural environments and in water treatment units⁶⁻¹⁰. Among the series of manganese oxides, Mn_3O_4 is particularly known to be an effective and

*e-mail: ciminelli@demet.ufmg.br

inexpensive catalyst in various oxidation and reduction reactions^{11,12}. The use of powder magnetic manganese oxide composites as adsorbents may combine the excellent adsorptive and oxidation properties of manganese oxide with good performance recovery of magnetic separation techniques. Nevertheless, very few works have been focusing on magnetic manganese oxide composites to be used in water treatment^{4,5}. Moreover, in these published works, the magnetic composites are often synthesized by precipitation of manganese oxide, when in presence of magnetite, by using relatively costly oxidants, such as potassium permanganate and hydrogen peroxide.

Considering the aforementioned context, the present work aims to synthesize low-cost magnetic Mn_3O_4 composites, with chemical stability and physical integrity, in stirred solid-aqueous systems. The magnetic sorbent is applied to As(III) removal in environmental systems.

2. Experimental

All chemicals were of analytical grade and used without further purification. All solutions were prepared with deionized water with a conductivity of $18.2 \mu\text{S}\cdot\text{cm}^{-1}$ obtained with a Milli-Q water purification system (Millipore). To remove contaminants that had been potentially adsorbed onto the glass and plastic walls, all vessels and instruments were cleaned by soaking in detergent solution, then in $1.0 \text{ mol}\cdot\text{L}^{-1}$ HNO_3 solution, and subsequently in deionized water, in each case for at least 24 hours. All parts of the spectroscopic equipment used to extract and fill the sample cells was cleaned and rinsed properly with acetone. The pH electrode (713 pH Meter, Metrohm) was calibrated everyday with three pH buffers (pH 4.0, 7.0, and 10.0).

2.1. Synthesis of the magnetic manganese oxide composite

For the preparation of the composite, 1000 mL of deionized water was placed in contact with 1.0 g of commercial magnetite particles (Sigma-Aldrich, $< 5 \mu\text{m}$) and 45 mL of $1.0 \text{ mol}\cdot\text{L}^{-1}$ $\text{MnCl}_2\cdot 4\text{H}_2\text{O}$ (Sigma-Aldrich) solution at pH 12 ($1.0 \text{ mol}\cdot\text{L}^{-1}$ KOH – Sigma-Aldrich) in a 2000 mL Pyrex beaker under stirring (mechanical stirrer, Fisatom 713 D) and constant air input (aquarium pump Power 500). This same reaction was also carried out in the absence of magnetite particles for comparison. The resulting solid were separated from the liquid by using a neodymium magnet ($180 \times 100 \times 35 \text{ mm}$, IMATEC PRODUTOS MAGNÉTICOS LTDA) and washed using deionized water. The solutions were analyzed by Atomic Absorption Spectrometry, AAS (Perkin Elmer Analyst A300), for iron and manganese content.

2.2. Evaluation of the sorbent chemical stability and physical integrity

The chemical stability of the composite is associated with the dissolution of solid constituents, while the physical integrity of the composite is associated with the coating detachment.

The chemical stability and physical integrity tests consisted of batch experiments in which 0.2 g of the

magnetic composite was placed in contact with 100 mL aqueous solutions in different pH values (from 2.0 to 12) in 250 mL Pyrex vessels sealed with laboratory parafilm (Pechiney plastic packaging, USA) and stirred for 24 hours in a thermostatic shaker (New Brunswick Scientific Edison, USA) at room temperature. The solid was separated from the solution by a neodymium magnet, while the supernatant solution was vacuum-filtered through a $0.22 \mu\text{m}$ membrane filter (Fisher Scientific). The membrane filters before and after filtration were weighed on a precision balance (Mettler AE 200) to estimate the coating detachment. The solution was analyzed by AAS for Mn and Fe contents, whereas the solids were analyzed by EDS for Mn and Fe contents. The tests were carried out in duplicate.

2.3. Spectroscopic and image analyses techniques

Raman spectroscopic and X-ray diffraction (XRD) analyses were carried out for solid identification. Raman spectra were collected on a Horiba Jobin Yvon LABRAM-HR 800 spectrograph, equipped with a 633 nm helium-neon laser, 20 mW of power, attached to an Olympus BHX microscope equipped with 10, 50, and 100X lenses. The diffractograms were obtained on a Philips-PANalytical PW 1710 X-ray diffractometer equipped with a texture chamber.

Transmission electron microscopy (TEM) images of the samples were obtained using a Tecnai – G2-20-FEI 2006 microscope. A Thermo Noram (Quest) spectrometer with energy dispersive X-ray analysis (EDS) was used for elemental detection.

X-ray absorption near-edge structure (XANES) spectra were obtained to determine arsenic oxidation states using the synchrotron facilities at the Laboratório Nacional de Luz Síncrotron (LNLS), in Campinas, Brazil, at the XAFS2 workstation in the transmission mode at room temperature using a Si (111) double crystal monochromator.

Mössbauer spectroscopy data were collected on a conventional constant acceleration Mössbauer spectrometer (Halder) in transmission mode with a ^{57}Co (Rh) source to identify the composite's magnetic phase.

Measurements of the specific surface area were taken by means of the BET (Brunauer-Emmett-Teller) – Multipoint method through nitrogen adsorption using a Quantachrome Autosorb-1.

2.4. Arsenic immobilization

In the batch arsenic sorption experiments, 0.2 g of the adsorbent material (magnetic composite or manganese oxide) was added into the 250 mL Pyrex erlenmeyers flasks, filled with 100 mL of As(III) solution at initial pH 5.0, and the vessels sealed with laboratory parafilm (Pechiney plastic packaging, USA). The As(III) stock solution was prepared by dissolving NaAsO_2 (Fluka) in Milli-Q water. Initial As(III) concentrations varied from 1.0 to $50 \text{ mg}\cdot\text{L}^{-1}$. Agitation at 200 rpm was provided by a thermostatic shaker (manufactured by New Brunswick Scientific Edison, USA). The temperature was maintained at $(25 \pm 0.5)^\circ\text{C}$. After 24 hours, the pH of the solutions was measured, and the samples were separated from the liquid by using a magnet.

The filtrate was directly assayed for total arsenic, iron and manganese using inductively coupled plasma optical emission spectrometry, ICP-OES (Perkin-Elmer Optima 7300 DV). The tests were carried out in duplicate.

3. Results and Discussion

3.1. Evaluation of the composite chemical stability and physical integrity

The supernatants obtained after the magnetic separation of the solid samples stirred in pH 10 and pH 12 aqueous solutions were turbid (brown yellow) and had to be vacuum-filtered twice through a $0.22\ \mu\text{m}$ membrane filter (Fisher Scientific) to achieve clarification. EDS results have shown the presence of only manganese in the fine filtrate particles, indicating that the physical integrity of the magnetic composite was compromised in these pH values (22% of Mn_3O_4 was separated from magnetite particles). When stirring at pH values from 3.0 to 9.0, no turbidity could be observed in the supernatants obtained after magnetic separation, which indicates that the physical integrity was preserved (less than 1% of Mn_3O_4 was separated from the magnetite particles). A significant manganese dissolution (49%) could only be observed in pH 2.0. In pH values from 3.0 to 9.0, less than 1% of manganese was dissolved. Iron dissolution was not detected ($< 10\ \mu\text{g}\cdot\text{L}^{-1}$).

It can be concluded that the composite has shown a good chemical stability and physical integrity in pH values ranging from 3.0 to 9.0, which is the commonly used range for arsenic adsorption in water treatment units.

3.2. Sorbent characterization

The values of specific surface areas for commercial magnetite, manganese oxide, and magnetic manganese oxide composite samples are 6, 54 and $39\ \text{m}^2\cdot\text{g}^{-1}$, respectively. The TEM image of the composite (Figure 1) shows dominantly octahedral morphology.

Figure 2 shows the XRD diagrams of the samples. The synthesis of Mn_3O_4 , in both the absence and presence of magnetite, can be confirmed by the presence of diffraction peaks corresponding to a tetragonal structure of Mn_3O_4 (JCPDS, 24-0734-hausmannite structure, I41/amd, with lattice constants $a = 5.746\ \text{\AA}$ and $c = 9.463\ \text{\AA}$). The diffraction peaks of pure Mn_3O_4 are broader than the diffraction peaks of the composite. This result indicates that the synthesis in the presence of magnetite favors the formation of a more ordered Mn_3O_4 material with a single phase of manganese oxide. The diffraction pattern of the composite has also shown some peaks which correspond to the diffraction pattern of commercial magnetite, as was expected from the bulk.

Raman spectra of the composite and manganese oxide (Figure 3) have confirmed the presence of Mn_3O_4 [13,14]. The Raman spectrum of bulk Mn_3O_4 (MnMn_2O_4 in spinel notation) is characterized by a very sharp peak at $654\ \text{cm}^{-1}$. This peak corresponds to the Mn-O breathing vibration of divalent manganese ions in tetrahedral coordination. Two smaller peaks are located at $300\text{--}310$ and $350\text{--}360\ \text{cm}^{-1}$. Bulk Mn_3O_4 also presents a weak signal at $485\ \text{cm}^{-1}$ [15].

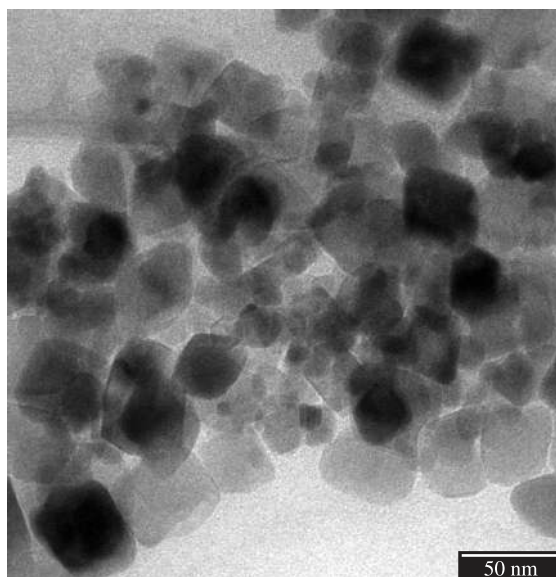


Figure 1. TEM image of the magnetic composite.

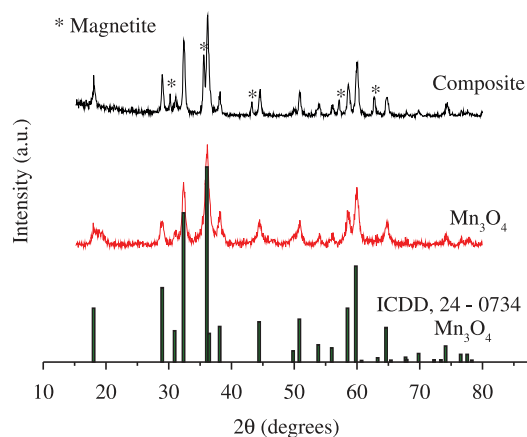


Figure 2. X-ray powder diffraction patterns of the magnetic composite and synthesized Mn_3O_4 sample and the main Bragg lines of hausmannite (Mn_3O_4 – ICDD 24-0734). The asterisk refers to magnetite (Fe_3O_4) diffraction peaks.

However, these values may shift to higher values as grain sizes decrease due to the phonon confinement effect¹⁶.

Mössbauer results show that the ratios of the areas of octahedral and tetrahedral sites of magnetite and the composite indicate oxidation from Fe(II) to Fe(III) (Table 1, Figure 4). However, the oxidation does not compromise magnetic separation.

3.3. Arsenic immobilization experiments

In the As(III) sorption experiments with the composite and manganese oxide samples, the pH values of the solutions increased from 5.0 to 7.0 and from 5.0 to 6.0, respectively, indicating that H^+ ions are being consumed. The As(III) sorption isotherms are shown in Figure 5. The maximum

sorption capacity and affinity of arsenic ions were evaluated from the isotherms by Langmuir (1), Freundlich (2) and combined Langmuir and Freundlich (3) models expressed as follows:

$$q = \frac{b q_m C_e}{1 + b C_e}$$

(1)

$$q = k C_e^{\left(\frac{1}{n}\right)}$$

(2)

$$q = \frac{b q_m C_e^{\left(\frac{1}{n}\right)}}{1 + b C_e^{\left(\frac{1}{n}\right)}}$$

(3)

where q is the amount of arsenic adsorbed per unit surface area of adsorbent (mmol.m^{-2}), C_e is the equilibrium concentration of arsenic (mg.L^{-1}), b is the constant related to the free energy of adsorption (L.mg^{-1}), q_m is the maximum adsorption capacity (mmol.m^{-2}), k is the Freundlich constant, indicative of the relative adsorption capacity of the adsorbent (mmol.m^{-2}), and $(1/n)$ is the adsorption intensity.

The isotherms best fitting results are listed in Table 2. The maximum sorption capacity is $14 \text{ mg}_{\text{As}} \text{ g}_{\text{solid}}^{-1}$ ($0.0048 \text{ mmol}_{\text{As}} \text{ m}^{-2}_{\text{solid}}$) for the composite and $20 \text{ mg}_{\text{As}} \text{ g}_{\text{solid}}^{-1}$ ($0.0049 \text{ mmol}_{\text{As}} \text{ m}^{-2}_{\text{solid}}$) for Mn_3O_4 sample. The values are comparable to the value (14.7 mg.g^{-1}) found for a raw material rich in Fe_2O_3 and MnO_2 with a specific surface area of $40.8 \text{ m}^2.\text{g}^{-1}$ ($0.0048 \text{ mmol}_{\text{As}} \text{ m}^{-2}_{\text{solid}}$)⁷, and are considered high when compared to other synthetic manganese dioxides found in the literature, such as birnessite ($\sim 0.0029 \text{ mmol}_{\text{As}} \text{ m}^{-2}_{\text{solid}}$), for the same range of initial arsenic concentration (less than 50 mg.L^{-1})⁹. The composite and the Mn_3O_4 sample have shown high and similar affinity for As(III). The similarity is associated with the good coating of the composite. High

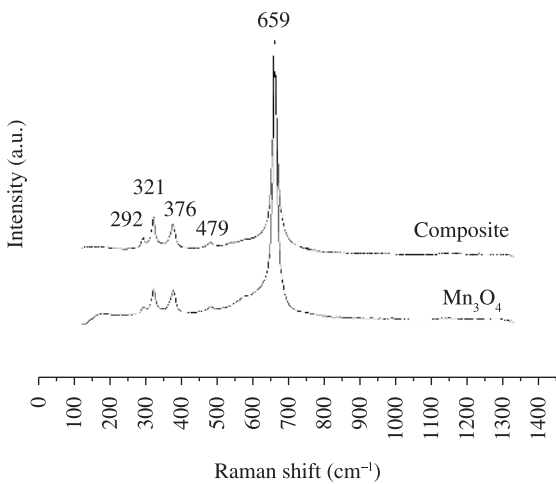


Figure 3. Raman spectra of the magnetic composite and synthesized Mn_3O_4 sample.

Table 1. Mössbauer hyperfine parameters of magnetite and magnetic composite.

Magnetite			Composite		
	mag (O)	mag (T)		mag (O)	mag (T)
IS (mm/s)	0.54	0.19	IS (mm/s)	0.55	0.2
QS (mm/s)	0.00	−0.02	QS (mm/s)	0.01	−0.02
B _{HF} (T)	45.78	49.22	B _{HF} (T)	45.79	49.34
Area (%)	53.3	46.7	Area (%)	55.53	44.47
A _{(O) / A_(T)}	1.14		A _{(O) / A_(T)}	1.25	

IS: isomer shift; QS: quadrupole splitting; B_{HF}: hyperfine field; T: tetrahedral sites; O: octahedral sites.

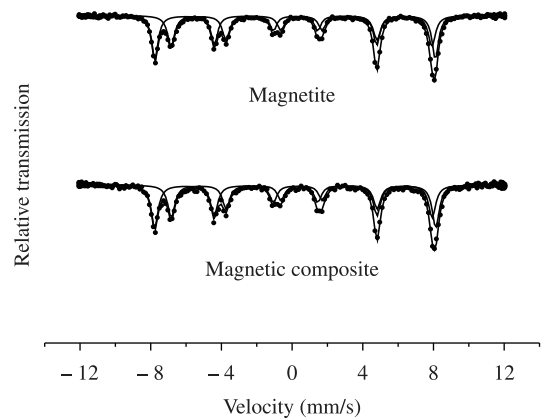


Figure 4. Mössbauer spectra of commercial magnetite and the magnetic composite measured at 300 K.

Table 2. Isotherm parameters for As(III) on the composite and Mn_3O_4 sample.

Sample	q_m (mmol.m^{-2})	b (L.mg^{-1})	Best model
Composite	(0.0048 ± 0.0003)	(1.7 ± 0.5)	Langmuir
Mn_3O_4	(0.0049 ± 0.0007)	(0.9 ± 0.4)	Langmuir

b: constant related to the free energy of adsorption; q_m : maximum adsorption capacity.

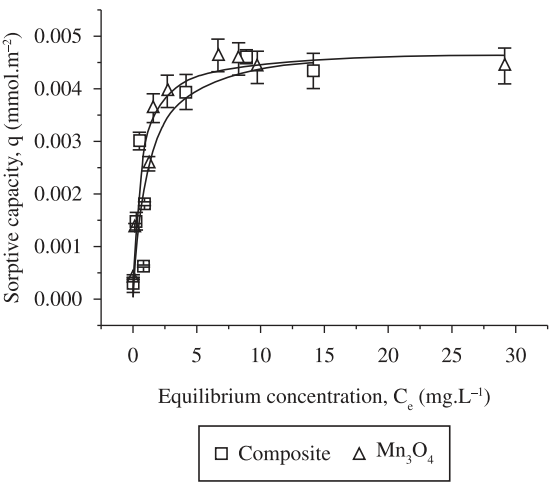
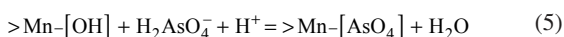
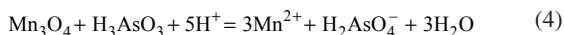


Figure 5. Isotherm for As(III) sorption on the magnetic composite and synthesized Mn_3O_4 sample. Experimental conditions: pH 5.0, 200 rpm, 24 hours, $(25 \pm 0.5)^\circ\text{C}$. Error bars represent the error calculated considering the equipment error of 5%.

affinity adsorbents are desired for the removal of trace and sub-trace contaminants, as is true in the removal of arsenic from water.

The reactions that would most likely occur during the sorption of arsenate in Mn_3O_4 tests are the oxidation of arsenite to arsenate and a reductive dissolution of Mn_3O_4 , in turn releasing Mn(II) into the solution (Equation 4) as well as causing the adsorption of arsenate ions onto hausmannite (Equation 5)⁹.



According to Equation 4, there should be three times more Mn released than As sorbed. Manganese and iron release were analysed during the sorption tests. Iron was not detected ($< 10 \mu\text{g.L}^{-1}$). A relation between Mn release and As sorption is shown in Figure 6. It can be seen that, in initial concentrations of above 20 mg.L^{-1} , there is more As

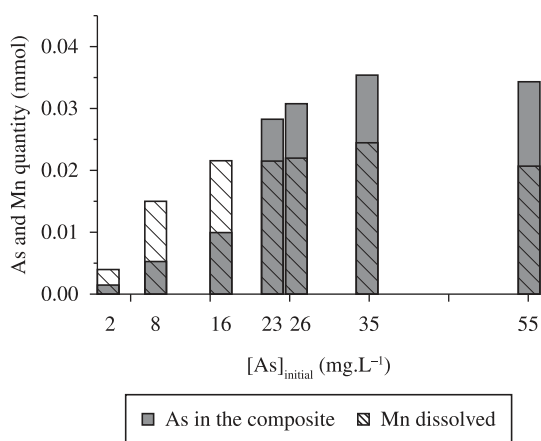


Figure 6. Relation between arsenic in the composite and Mn in solution.

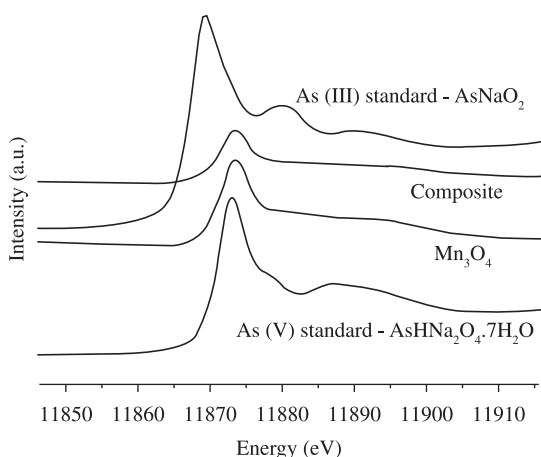


Figure 7. Room temperature XANES spectra of the composite, synthesized Mn_3O_4 sample, and As(III) and As(V) standards (AsNaO_2 and $\text{AsHNa}_2\text{O}_4 \cdot 7\text{H}_2\text{O}$, respectively).

sorbed than Mn released. Figure 7 compares the As K-edge XANES spectra of the composite and Mn_3O_4 sample after arsenic removal tests with arsenic salts used as standards, indicating that all As adsorbed is in the oxidized arsenic form, As(V). Therefore, it can be concluded that part of the Mn(II) in solution is being adsorbed or precipitated, or both. This will be confirmed by ongoing Raman and Extended X-ray Absorption Fine Structure (EXAFS) analyses.

Mechanisms of As(III) oxidation by Mn-oxides can be quite complex, involving several simultaneous reactions. Some investigations suggest that the oxidation of As(III) to As(V) using manganese dioxide involves the reduction of Mn(IV) to Mn(III), followed by Mn(III) to Mn(II), consistent with one electron transfer reactions^{9,17-20}. Many works on the complexation of arsenite and arsenate by manganese dioxide using XAFS show that As(III) is oxidized to As(V), while only arsenate is adsorbed onto MnO_2 surfaces²⁰⁻²². The majority of these works show that arsenate is adsorbed on the edge of MnO_2 , binding to the Mn(IV) octahedron in bidentate binuclear form^{20,21}. A more recent work has shown that arsenate can bind to the Mn(IV) octahedron in both monodentate mononuclear and bidentate binuclear forms, as well as to the Mn(III) octahedron in both monodentate mononuclear and bidentate mononuclear forms²³. A work from our group has shown that during As(III) sorption onto a manganese dioxide (Na-birnessite , $\text{Na}_{0.55}\text{Mn}_2\text{O}_4 \cdot 1.5\text{H}_2\text{O}$), hausmannite (Mn_3O_4) is the intermediate product of reductive dissolution of manganese dioxide, whereas arsenate is adsorbed by Mn_3O_4 . Moreover, it has been demonstrated that the precipitation of a Mn(II) arsenate, $\text{Mn}_3(\text{AsO}_4)_2 \cdot 4\text{H}_2\text{O}$, occurs for high arsenic concentrations (above 160 mg.L^{-1})⁹. However, no detailed study has been carried out to show how arsenic is complexed on the surface of hausmannite.

4. Conclusions

The results of the synthesis of manganese oxide (Mn_3O_4) coated magnetite have demonstrated that stable magnetic adsorbents with high affinity for As(III) solutions can be generated.

The composite has shown a good chemical stability and physical integrity in pH values ranging from 3.0 to 9.0, which is commonly used range for arsenic adsorption in water treatment units.

Magnetic Mn_3O_4 composites have shown high affinity for arsenic and represent a practical approach to the separation of arsenic from water. All As adsorbed onto the composite was in oxidized arsenic form, As(V). Moreover, the magnetic property of magnetite, which is attached to the active Mn_3O_4 , allows for the removal of the sorbent particles from the solution.

Acknowledgements

We would like to thank CNPq, Fapemig, CAPES and INCT on Mineral Resources Water, Mineral Resources and Biodiversity for their financial support. We would also like to thank Ms Andréia Bicalho (DEMIN-UFMG) for XRD analyses, Ms Ilda de Sousa (DEMET-UFMG) for BET results, Dr. Pablo Muñoz (GMMA-CBPF) for Mössbauer measurements and the Center of Microscopy at the Universidade Federal de Minas Gerais (CM-UFMG) for TEM images and LNLS for XANES measurements.

References

1. Mohan D and Pittman Junior CU. Arsenic removal from water/wastewater using adsorbents-A critical review. *Journal of Hazardous Materials*. 2007; 142:1-53. PMID:17324507. <http://dx.doi.org/10.1016/j.jhazmat.2007.01.006>
2. Yavuz CT, Mayo JT, Yu WW, Prakash A, Falkner JC, Yean S et al. Low-Field Magnetic Separation of Monodisperse Fe_3O_4 Nanocrystals. *Science*. 2006; 314:964-967. PMID:17095696. <http://dx.doi.org/10.1126/science.1131475>
3. Qu J. Research progress of novel adsorption processes in water purification: A review. *Journal of Environmental Sciences*. 2008; 20:1-13. [http://dx.doi.org/10.1016/S1001-0742\(08\)60001-7](http://dx.doi.org/10.1016/S1001-0742(08)60001-7)
4. Rosas CAC, Franzreb M, Valenzuela F and Höll WH. Magnetic manganese dioxide as an amphoteric adsorbent for removal of harmful inorganic contaminants from water. *Reactive & Functional Polymers*. 2010; 70:516-520. <http://dx.doi.org/10.1016/j.reactfuncpolym.2010.03.011>
5. Chen H, Chu PK, He J, Hu T and Yang M. Porous magnetic manganese oxide nanostructures: Synthesis and their application in water treatment. *Journal of Colloid and Interface Science*. 2011; 359:68-74. PMID:21507410. <http://dx.doi.org/10.1016/j.jcis.2011.03.089>
6. Smedley PL and Kinniburgh DG. A review of the source, behavior and distribution of arsenic in natural waters. *Applied Geochemistry*. 2002; 17(5):517-568. [http://dx.doi.org/10.1016/S0883-2927\(02\)00018-5](http://dx.doi.org/10.1016/S0883-2927(02)00018-5)
7. Deschamps E, Ciminelli VST and Höll WH. Removal of As(III) and As(V) from water using a natural Fe and Mn enriched sample. *Water Research*. 2005; 39(20):5212-5220. PMID:16290184. <http://dx.doi.org/10.1016/j.watres.2005.10.007>
8. Ladeira AC and Ciminelli VST. Adsorption and desorption of arsenic on an oxisol and its constituents. *Water Research*. 2004; 38:2087-2094. PMID:15087189. <http://dx.doi.org/10.1016/j.watres.2004.02.002>
9. Vaclavikova M, Gallios GP, Hredzak S and Jakabsky S. Removal of arsenic from water streams: an overview of available techniques. *Clean Technologies and Environmental Policy*. 2008; 10:89-95.
10. Dias A, Sa RG, Spitale MC, Athayde M and Ciminelli VST. Microwave-hydrothermal synthesis of nanostructured Nabirnessites and phase transformation by arsenic(III) oxidation. *Materials Research Bulletin*. 2008; 43:1528-1538. <http://dx.doi.org/10.1016/j.materresbull.2007.06.019>
11. Parsons JG, Lopez ML, Peralta-Videa JR and Gardea-Torresdey JL. Determination of arsenic(III) and arsenic(V) binding to microwave assisted hydrothermal synthetically prepared Fe_3O_4 , Mn_3O_4 , and MnFe_2O_4 nanoadsorbents *Microchemical Journal*. 2009; 91:100-106. <http://dx.doi.org/10.1016/j.microc.2008.08.012>
12. Zhang H, Liang C, Tian Z, Wang G and Cai W. Single Phase Mn_3O_4 Nanoparticles Obtained by Pulsed Laser Ablation in Liquid and Their Application in Rapid Removal of Trace Pentachlorophenol. *Journal of Physical Chemistry C*. 2010; 114:12524-12528.
13. Han YF, Chen FX, Zhong ZY, Ramesh K, Chen LW and Widjaja E. Controlled Synthesis, Characterization, and Catalytic Properties of Mn_2O_3 and Mn_3O_4 Nanoparticles Supported on Mesoporous Silica SBA-15. *Journal of Physical Chemistry B*. 2006; 110:24450-24456. PMID:17134200. <http://dx.doi.org/10.1021/jp064941v>
14. Tian ZR, Tong W, Wang JY, Duan NG, Krishnan VV and Suib SL. Manganese Oxide Mesoporous Structures: Mixed-Valent Semiconducting Catalysts. *Science*. 1997; 276:926-929. <http://dx.doi.org/10.1126/science.276.5314.926>
15. Julien CM, Massot M and Poinignon C. Lattice vibrations of manganese oxides Part I. Periodic structures. *Spectrochimica Acta Part A*. 2004; 60(3):689-700. [http://dx.doi.org/10.1016/S1386-1425\(03\)00279-8](http://dx.doi.org/10.1016/S1386-1425(03)00279-8)
16. Xu HY, Xu SL, Wang H and Yan H. Characterization of Hausmannite Mn_3O_4 Thin Films by Chemical Bath Deposition. *Journal of The Electrochemical Society*. 2005; 152(12):C803-C807. <http://dx.doi.org/10.1149/1.2098267>
17. Driehaus W, Seith R and Jekel M. Oxidation of arsenate(III) with manganese oxides in water treatment. *Water Research*. 1994; 29(1):297-305. [http://dx.doi.org/10.1016/0043-1354\(94\)E0089-O](http://dx.doi.org/10.1016/0043-1354(94)E0089-O)
18. Scott MJ and Morgan JJ. Reactions at Oxide Surfaces. 1. Oxidation of As(III) by Synthetic Birnessite. *Environmental Science & Technology*. 1995; 29:1898-1905. <http://dx.doi.org/10.1021/es00008a006>
19. Nesbitt HW, Canning GW and Bancroft GM. XPS study of reductive dissolution of 7Å-birnessite by H_3AsO_3 , with constraints on reaction mechanism. *Geochimica et Cosmochimica Acta*. 1998; 62(12):2097-2110. [http://dx.doi.org/10.1016/S0016-7037\(98\)00146-X](http://dx.doi.org/10.1016/S0016-7037(98)00146-X)
20. Manning BA, Fendorf SE, Bostick B and Suarez DL. Arsenic(III) Oxidation and Arsenic(V) and Adsorption Reactions on Synthetic Birnessite. *Environmental Science & Technology*. 2002; 36:976-981. <http://dx.doi.org/10.1021/es0110170>
21. Foster AL, Brown Junior GE and Parks GA. X-ray absorption fine structure study of As(V) and Se(IV) sorption complexes on hydrous Mn oxides. *Geochimica et Cosmochimica Acta*. 2003; 67(11): 1937-1953.
22. Lafferty BJ, Ginder-Vogel M, Zhu M, Livi KJ and Sparks DL. Arsenite Oxidation by a Poorly Crystalline Manganese-Oxide. 2. Results from X-ray Absorption Spectroscopy and X-ray Diffraction *Environmental Science & Technology*. 2010; 44:8467-8472. <http://dx.doi.org/10.1021/es102016c>